Capture of an impurity by a vortex line in a Bose condensate

Natalia G. Berloff* and Paul H. Roberts†
Department of Mathematics, University of California, Los Angeles, California 90095-1555
(Received 23 June 2000; published 20 December 2000)

The Bose condensate model is used to elucidate the interaction of vortex lines with impurities. Three-dimensional numerical integration of the coupled nonlinear Schrödinger equations, which describe the evolution of the wave functions of the Bose condensate and an impurity, are used to study the process of capture of the impurity by a rectilinear vortex and to elucidate the binding energy. Kelvin waves are generated during capture.

DOI: 10.1103/PhysRevB.63.024510 PACS number(s): 67.55.Fa, 47.20.Ky, 02.60.Cb, 05.45.−a

Much of what is known about vortices in superfluid helium is obtained from experiments using impurities as probes. These impurities are of three types: negative ions, which are electrons in relatively large (radius ~16 Å) bubbles cut out of the liquid owing to the repulsive interactions between helium atoms and electrons; positive ions such as $^4He_2^+$ (~8 Å); and neutral atoms such as ^{3}He (~4 Å).

Rayfield and Reif[1] used an ion time-of-flight spectrometer to determine the dynamics of ion-quantized vortex ring complexes. They observed that above some critical velocity v_c, ideal superflow around an ion breaks down. The moving ion produces vortex rings and the ion becomes trapped in one of these. The capture of negative ions by quantized vortex lines in a rotating bucket was first demonstrated by Careri *et al.*[2]

The dynamics of a Bose condensate is accurately described by the Gross-Pitaevskii (GP) model.[3] This equation was successfully used to elucidate qualitatively the motion of vortex rings,[4] the nucleation of vortex rings by moving bodies,[5,6] and the reconnection of vortex lines.[7] The main problem we address in this paper is the capture of ions by vortex lines.

Consider first the negative ion or ''electron bubble.'' In the Hartree approximation, the equations governing the one-particle wave function of the condensate, ψ, and the wave function of the impurity, ϕ, are a pair of coupled equations suggested by Gross[8] and by Clark:[8]

$$\mathrm{i}\hbar\frac{\partial\psi}{\partial t}=-\frac{\hbar^2}{2M}\nabla^2\psi+(U_0|\phi|^2+V_0|\psi|^2-E)\psi, \tag{1}$$

$$\mathrm{i}\hbar\frac{\partial\phi}{\partial t}=-\frac{\hbar^2}{2\mu}\nabla^2\phi+(U_0|\psi|^2-E_e)\phi, \tag{2}$$

where M and E are the mass and single-particle energy for the bosons; μ and E_e are the mass and energy of the electron. The interaction potentials between bosons and electrons and between bosons are here assumed to be of δ-function form $U_0\delta(\mathbf{x}-\mathbf{x}')$ and $V_0\delta(\mathbf{x}-\mathbf{x}')$, respectively. To lowest order, perturbation theory predicts such interaction potentials to be $U_0=2\pi l\hbar^2/\mu$ and $V_0=4\pi d\hbar^2/M$, where l is the boson-impurity scattering length, and d is the boson diameter. The normalization conditions on the wave functions are

$$\int|\psi|^2dV=N,\quad \int|\phi|^2dV=1, \tag{3}$$

where N is the total number of bosons in the system. The healing length is defined by $a=\hbar(2\rho_sV_0)^{-1/2}=(8\pi d\psi_\infty^2)^{-1/2}$, where $\rho_s=M\psi_s^2=EM/V_0$ is the mean condensate mass density.

Using the system (1), (2), Grant and Roberts[9] studied the motion of a negative ion moving with speed v using an asymptotic expansion in v/c, where c is the speed of sound, so that their leading order flow is incompressible. Treating $\epsilon\equiv(a\mu/lM)^{1/5}$ as a small parameter they calculated the effective (hydrodynamic) radius and effective mass of the electron bubble. We choose a nondimensionalization of Eqs. (1) and (2) different from theirs; we use a as our unit of length $\mathbf{x}\to a\mathbf{x}$, $t\to(a^2M/\hbar)t$, $\psi\to\psi_\infty\psi$, and $\phi\to(\epsilon^3/4\pi a^3)^{1/2}\phi$, so that

$$2i\frac{\partial\psi}{\partial t}=-\nabla^2\psi+(|\psi|^2+f|\phi|^2-1)\psi, \tag{4}$$

$$2i\delta\frac{\partial\phi}{\partial t}=-\nabla^2\phi+(q^2|\psi|^2-k^2)\phi, \tag{5}$$

where $q^2=l/2d, \delta=\mu/M, k^2=\mu E_e/ME$ and $f=1/\epsilon^2$. Taking $\rho_s=145.2\ \mathrm{kg\,m^{-3}}$, we see that $\psi_\infty\approx0.148\ \text{Å}^{-3/2}$ and $E/V_0\approx0.0218\ \text{Å}^{-3}$. If $a=1$ Å, then $V_0\approx0.024\ \mathrm{eV}\,\text{Å}^3$ and $d\approx1.82$ Å and $E\approx5.22\times10^{-4}$ eV. Assuming $l=0.6$ Å, we find that $\epsilon=0.187$, $q=0.41$, $f=28.6$, and $U_0\approx28.7\ \mathrm{eV}\,\text{Å}^3$. Since $E_e\approx0.13$ eV, $k=0.185$. The normalization condition on ϕ becomes $\int|\phi|^2dV=4\pi/\epsilon^3$.

The nondimensionalization makes it plain that k,ϵ (and of course $\delta=1.4\times10^{-4}$) are small, and suggests how approximate solutions to Eqs. (4) and (5) may be found. Except within the condensate and within a healing layer at the bubble surface of thickness 1 much less than the bubble radius, ψ is negligible in Eq. (5) and, since $\delta\ll1$, this reduces at leading order to the Helmholtz equation $\nabla^2\phi+k^2\phi=0$, which in spherical coordinates (r,θ,χ) has the solution

$$\phi=(k^3/\pi\epsilon^3)^{1/2}\sin(kr)/kr, \tag{6}$$

which is appropriate for a motionless bubble, and shows that the dimensionless radius b of that bubble is $b=\pi/k\approx17$, or

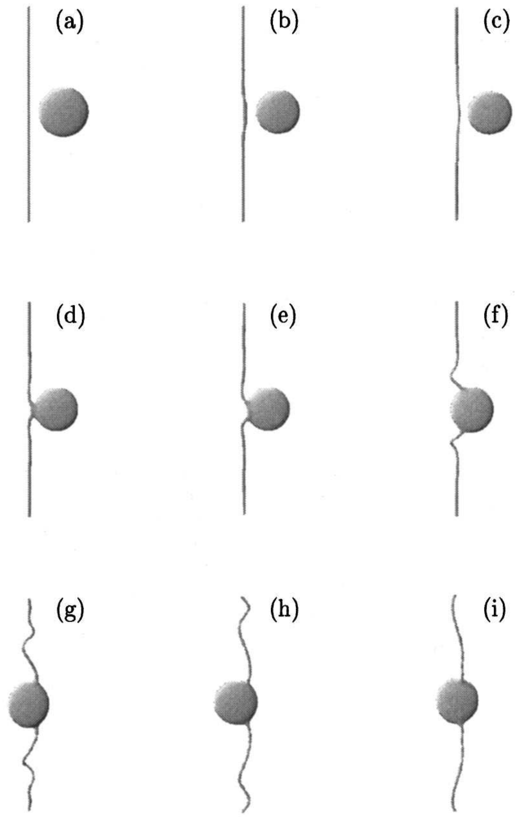

FIG. 1. The results of numerical integration of Eqs. (4) and (5) for the negative ion initially placed a distance $6a$ apart from the rectilinear vortex line. The pictures show the isosurface $\rho=0.2\rho_\infty$ at (a) $t=0$, (b) $t=16.6a/c$, (c) $t=96a/c$, (d) $t=146.6a/c$, (e) $t=156a/c$, (f) $t=200a/c$, (g) $t=263a/c$, (h) $t=323a/c$, and (i) $t=413a/c$.

17 Å in physical units, which, being much greater than a, justifies the asymptotic approach through which we derive our solution.

A vortex in the condensate is a line (or curve) on which the complex field ψ is zero and round which its phase increases by 2π, which is also the circulation of the flow $\mathbf{u}$ of condensate about the line on curve. The Bernoulli effect of the flow propels the ion and vortex towards one another with a force approximately proportional to s^{-3}, where s is the closest distance between them.[10]

To observe and elucidate the process of capture of the impurity by the vortex line we solved Eqs. (4) and (5) by modifying our finite-differences code previously used to solve the GP model of the flow around the moving ion.[6] See Ref. 11 for details. Initially the impurity was placed at a distance of 6 healing lengths from the vortex line. The process of capture is clearly seen in Fig. 1. What came as a surprise is that this process can be better characterized as the reconnection of the vortex line with its pseudoimage inside the impurity. Initially the vortex line bends towards the impurity at the point where the distance between them is least. As a result of this interaction the impurity moves around the vortex axis. The process of capture continues as the vortex line terminates on the surface of the impurity and its feet move to opposite poles of the impurity surface. At the same time helical waves start propagating from the impurity along the two segments of the vortex line. Such helical waves have been observed during the relaxation of the vortex angle when two vortex lines reconnect,[12] and are just Kelvin waves.

During the time in which the vortex merges with the healing layer round the ion [the layer of thickness $\sim a$ in which neither ϕ in Eq. (4) nor ψ in Eq. (5) can be neglected], the character of the solution alters rapidly, corresponding to the topological change that defines the capture of the ion by the vortex. Once the vortex has divided into two, with separate feet attached to the healing layer, the flow around the ion has acquired a circulation that it previously could not possess.

The motion of the curved vortex line can be described using the local induction approximation $\partial\mathbf{s}/\partial t=\beta\partial\mathbf{s}/\partial\xi\times\partial^2\mathbf{s}/\partial\xi^2$, where $\mathbf{s}=\mathbf{s}(\xi,t)$ is the position vector of the vortex element labeled by arc length ξ along the vortex and $\beta=(\kappa/4\pi)\ln(L/a)$, where L is a cutoff distance. This approximation can be transformed[13] into the nonlinear Schrödinger equation

$$i\frac{\partial\varphi}{\partial t}=\frac{\partial^2\varphi}{\partial\xi^2}-\frac{1}{2}|\varphi|^2\varphi, \tag{7}$$

for $\varphi=\zeta\exp[i\int_0^\xi\tau d\xi']$, where ζ is the filament curvature, τ is torsion; ξ has been rescaled to ξ/a and t to $t\beta$. In Ref. 14 it was observed that the generation of Kelvin waves as the result of the reconnection of the vortex lines is a consequence of the conservation of the constants of motion I_n, given by $I_n=\int_{-\infty}^{\infty}f_n(\xi)d\xi$, $f_1=\frac{1}{4}|\varphi|^2$, and $f_{n+1}=\varphi(f_n/\varphi)'+\Sigma_{n_1+n_2=n}\ f_{n_1}f_{n_2}$. Since the interaction with the impurity increases the radius of curvature of the vortex line, the conservation of these constants of motion would be impossible without the emission of Kelvin waves. As the emitted Kelvin waves (left and right antikinks) propagate from the feet of the vortex lines to infinity radiating energy as they go, the impurity moves towards the center of the computational box and its center moves towards the axis of the straightening vortex line. Due to the circulation around the ion, the bubble surface is slightly flattened into a roughly prolate spheroidal form. There is no distortion in the final, steady-state configuration shown in Fig. 2. The electron wave function does not penetrate far along the vortex cores.

Schwarz and Donnelly[15] have observed that at low temperatures (<0.5 K) the straight-line vortices also can trap positive ions. When the Kelvin waves have radiated to infinity and the impurity has become situated symmetrically on the core, it supplants a substantial volume of high-velocity circulating fluid; the resulting lowering of the energy of the system is referred to as the ‘‘substitution energy’’ or sometimes as the ‘‘binding energy.’’ Donnelly and Roberts[16] used a healing model of the vortex core and estimated the substitution energy as

$$\Delta V=-2\pi\rho_s(\hbar/M)^2b[1-(1+a^2/b^2)^{1/2}\sinh^{-1}(b/a)]. \tag{8}$$

In what follows, we shall recalculate the substitution energy for positive and negative ions using the condensate model.

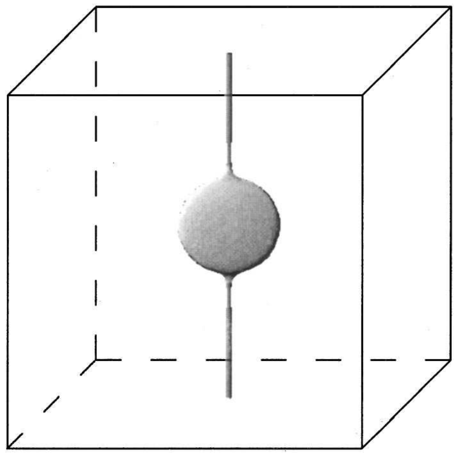

FIG. 2. The results of numerical integration of Eqs. (4) and (5) for the electron initially placed at the center of the rectilinear vortex line. The picture shows the isosurface $\rho = 0.2\rho_\infty$.

In the final steady state, $\psi = R(s,z)\exp(i\chi)$. If the positive ion is modeled as an infinite potential barrier, R vanishes on $s=0$ and on $r=b$; in $r>b$, it obeys

$$\frac{\partial^2 R}{\partial s^2} + \frac{1}{s}\frac{\partial R}{\partial s} + \frac{\partial^2 R}{\partial z^2} + \left(1 - \frac{1}{s^2}\right) R - R^3 = 0, \tag{9}$$

where R is scaled by R_∞ and length is scaled by a. This equation was used in Ref. 17 to determine the structure of a rectilinear filament standing perpendicularly on a flat inert boundary. The difference in the line energy with and without the vortex was calculated. Close to the boundary the vortex core energy becomes negative, which led to the conjecture that a passive vortex layer would necessarily exist at the wall. We performed similar calculations for the positive ion-vortex complex. It was numerically convenient, following Huepe and Brachet,[19] to replace the infinite potential barrier for the ion by $V_0 = -5[\tanh\{4(r-b)\} - 1]$, so that the $1 - V_0(r)$ appears instead of 1 in Eq. (9). It is then necessary to insist only that $R(0,z)=0$. When the difference of the energy densities of the vortex-ion complex and the ion without vortex is integrated over a constant z plane up to $r=L$, the energy density per unit length is obtained (in dimensional units) as

$$\mathcal{E}(z) = \frac{\rho\kappa^2}{4\pi}\left(\ln\frac{L}{a} + L_0(z)\right), \tag{10}$$

where $L_0 \to 0.38$ far from the ion.[18] Figure 3(a) shows L_0 for $z>0$ when a positive ion is present; the results for $z<0$ are identical. As in Ref. 17 the vortex core energy becomes negative close to the boundary of the ion, but this is a result of the larger depletion of the vortex core created by the boundary layer around the ion and does not imply the existence of a vorticity layer.

The final steady state for the electron bubble-vortex complex satisfies

$$\frac{\partial^2 R}{\partial s^2} + \frac{1}{s}\frac{\partial R}{\partial s} + \frac{\partial^2 R}{\partial z^2} + \left(1 - \frac{1}{s^2} - f\phi^2\right) R - R^3 = 0, \tag{11}$$

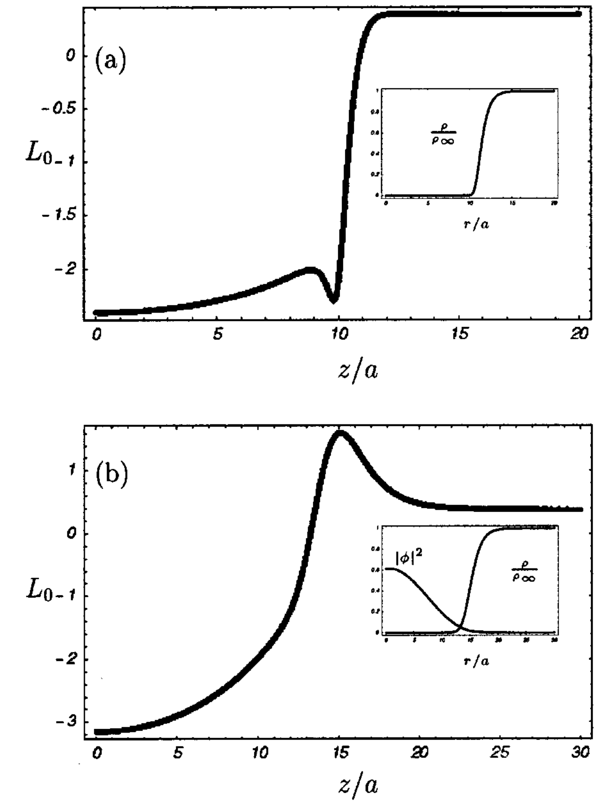

FIG. 3. The plot of the vortex core energy of (a) the positive ion-vortex complex and (b) the electron-vortex complex. Distance z is measured from the center of the impurity. The positive ion is of radius $10a$ in units of healing length a. The core energy L_0 per unit length is in units of $\rho\kappa^2/4\pi$. The insets show ρ/ρ_∞ and $|\phi|^2$ in units of $\epsilon^3/4\pi a^3$ as functions of r in the absence of a vortex.

$$\frac{\partial^2 \phi}{\partial s^2} + \frac{1}{s}\frac{\partial \phi}{\partial s} + \frac{\partial^2 \phi}{\partial z^2} + (k^2 - q^2 R^2)\phi = 0. \tag{12}$$

The plot of the vortex core energy as a function of the distance from the center of the electron bubble is given in Fig. 3(b). The substitution energy ΔV is the difference between the energy of the complex and the sum of the energies of the vortex and the ion when they are still remote from one another prior to capture. This gives

$$\Delta V = \frac{\rho\kappa^2 a}{2\pi}\int_0^\infty [L_0(z) - 0.38]\,dz. \tag{13}$$

The calculated substitution energy for the positive ion of radius $10a$ is 21.7 K if we use the nondimensionalization based on the speed of sound, so that $a=0.47$ Å; the expression (8) gives 15.8 K. If instead $a=1$ Å is used, we obtain $\Delta V/k_B \approx 46$ K, which may be compared with 33.5 K according to Eq. (8). For the electron bubble our result is $\Delta V/k_B = 55$ K, and Eq. (8) gives $\Delta V/k_B = 66$ K if $R = 16$ Å is used. Notice that the healing layers around the positive and negative ions differ dramatically; see the insets of Fig. 3. Also the healing layer close to the vortex feet is less depleted, which was not taken into account by Eq. (8). This, we believe, explains why Eq. (8) overestimates ΔV for the electron bubble.

In this paper we used the Bose condensate model to study the capture of impurities by straight-line vortices. This process has served as the basis for nearly all experiments with large quantized vortex rings and with vortex arrays in rotating containers. The present work was carried out at much the same time as that of Winiecki and Adams,[22] on the capture of a penetrable positive ion by a vortex ring, and of our own simulation of the capture of a negative ion by a vortex ring.[23]

This work was supported by NSF Grant No. DMS-9803480.

---

*Electronic address: nberloff@math.ucla.edu
†Electronic address: roberts@math.ucla.edu

[1] G.W. Rayfield and F. Reif, Phys. Rev. **136**, A1194 (1964).
[2] G. Careri, W.D. McCormick, and F. Scaramuzzi, Phys. Lett. **1**, 61 (1962).
[3] V.L. Ginzburg and L.P. Pitaevskii, Zh. Éksp. Teor. Fiz. **34**, 1240 (1958) [Sov. Phys. JETP **7**, 858 (1958)]; E.P. Gross, Nuovo Cimento **20**, 454 (1961).
[4] C.A. Jones and P.H. Roberts, J. Phys. A **15**, 2599 (1982).
[5] T. Frisch, Y. Pomeau, and S. Rica, Phys. Rev. Lett. **69**, 1644 (1992); T. Winiecki, J.F. McCann, and C.S. Adams, *ibid.* **82**, 5186 (1999).
[6] N.G. Berloff and P.H. Roberts, J. Phys. A **33**, 4025 (2000).
[7] J. Koplik and H. Levine, Phys. Rev. Lett. **71**, 1375 (1993); **76**, 4745 (1996).
[8] E.P. Gross, in *Quantum Fluids*, edited by D.B. Brewer (North-Holland, Amsterdam, 1966); R.C. Clark, Phys. Lett. **16**, 42 (1965); in *Superfluid Helium*, edited by J.F. Allen (North Holland, Amsterdam, 1966).
[9] J. Grant and P.H. Roberts, J. Phys. A **7**, 260 (1974).
[10] R.J. Donnelly, *Quantized Vortices in Helium II* (Cambridge University Press, Cambridge, England, 1991).
[11] To produce Fig. 1 we used the Raymond-Kuo open boundary condition (Ref. 20) on the sides parallel to the vortex line to allow the sound waves to escape from the integration box and the reflective boundaries on the side normal to the direction of the vortex line. In time stepping, the leapfrog scheme was implemented with a backward Euler step every 100 steps to prevent the even-odd instability. In space we used a fourth-order finite-difference scheme together with a second-order scheme close to the open boundary for both condensate and electron wave functions. Because of the smallness of δ, 50 time steps were taken in advancing ϕ before the next time step for ψ was performed. A numerical integration with a larger number of time steps in the impurity equation produced the same result. To minimize the numerical dispersion and to account for a small amount of normal fluid present in superfluid even at very low temperature a small dissipative term was added to Eq. (4); see Ref. 21 for details. The initial condition was chosen as $\psi(\mathbf{x},t=0)=\psi_1(\mathbf{x})\psi_2(\mathbf{x})$, where ψ_1 is the wave function of the rectilinear vortex directed along the y axis ($x=0$, $z=0$) and ψ_2 is the wave function of the condensate around the stationary impurity of radius $b=15$ centered at $\mathbf{x}_B=(b+6,0,0)$, so that $\psi_2=0$ for $|\mathbf{x}-\mathbf{x}_B|<b$ but $\psi_2=\tanh(|\mathbf{x}-\mathbf{x}_B|/\sqrt{2})$ otherwise. The initial condition for the impurity wave function was taken as in Eq. (6) centered at $\mathbf{x}_B$. The size of the computation box was $[-50,50]\times[-125,125]\times[-50,50]$ with a computational grid of $200\times500\times200$ points. Figure 1 shows part of computational volume with a z extent of $[-70,70]$. The code was tested against the asymptotic solutions of Ref. 9. The numerical scheme does not conserve energy but the dissipation of energy is very small. When the reflective boundary conditions were used instead of the radiative ones, the energy loss due to the dissipative character of the scheme did not exceed 10^{-3}% per 1000 time steps.
[12] F.R. Hama, Phys. Fluids **5**, 1156 (1962).
[13] H. Hasimoto, J. Fluid Mech. **51**, 477 (1972).
[14] B.V. Svistunov, Phys. Rev. B **52**, 3647 (1995).
[15] K.W. Schwarz and R.J. Donnelly, Phys. Rev. Lett. **17**, 1088 (1966).
[16] R.J. Donnelly and P.H. Roberts, Proc. R. Soc. London, Ser. A **312**, 519 (1969).
[17] S. Burkhart, M. Bernard, O. Avenel, and E. Varoquaux, Phys. Rev. Lett. **72**, 380 (1994).
[18] L.P. Pitaevskii, Zh. Éksp. Teor. Fiz. **40**, 646 (1961) [Sov. Phys. JETP **13**, 451 (1961)].
[19] C. Huepe and M.E. Brachet, C.R. Acad. Sci., Ser. III **325**, 195 (1997).
[20] W.H. Raymond and H.L. Kuo, Q.J.R. Meteorol. Soc. **110**, 535 (1984).
[21] N.G. Berloff, J. Low Temp. Phys. **116**, 359 (1999).
[22] T. Winiecki and C. S. Adams, cond-mat/0006125 (unpublished).
[23] N.G. Berloff and P.H. Roberts, J. Phys. A (to be published).